Pathological tremors: Deterministic chaos or nonlinear stochastic oscillators?

J. Timmer[a)]
Freiburger Zentrum für Datenanalyse und Modellbildung, Eckerstrasse 1, 79104 Freiburg, Germany and Fakultät für Physik, Hermann-Herder-Strasse 3, 79104 Freiburg, Germany

S. Häussler
Freiburger Zentrum für Datenanalyse und Modellbildung, Eckerstrasse 1, 79104 Freiburg, Germany and Fakultät für Physik, Hermann-Herder-Strasse 3, 79104 Freiburg, Germany and Neurologische Universitätsklinik Freiburg, Breisacher Strasse 64, 79110 Freiburg, Germany

M. Lauk
Freiburger Zentrum für Datenanalyse und Modellbildung, Eckerstrasse 1, 79104 Freiburg, Germany and Fakultät für Physik, Hermann-Herder-Strasse 3, 79104 Freiburg, Germany

C.-H. Lücking
Neurologische Universitätsklinik Freiburg, Breisacher Strasse 64, 79110 Freiburg, Germany

(Received 17 May 1999; accepted for publication 15 October 1999)

Pathological tremors exhibit a nonlinear oscillation that is not strictly periodic. We investigate whether the deviation from periodicity is due to nonlinear deterministic chaotic dynamics or due to nonlinear stochastic dynamics. To do so, we apply various methods from linear and nonlinear time series analysis to tremor time series. The results of the different methods suggest that the considered types of pathological tremors represent nonlinear stochastic second order processes. Finally, we evaluate whether two earlier proposed features capturing nonlinear effects in the time series allow for a discrimination between two pathological forms of tremor for a much larger sample of time series than previously investigated. © *2000 American Institute of Physics.*
[S1054-1500(00)01801-2]

The field of nonlinear dynamics introduced the fascinating idea that an apparently random behavior of a time series might have been generated by a low-dimensional chaotic deterministic dynamical system. For time series of two types of pathological tremor, we investigate if the underlying dynamics should be regarded as chaotic or nonlinear stochastic oscillatory processes. The key question for a distinction is the order of the process. Chaotic processes are of at least third order, while nonlinear stochastic oscillatory processes can be of second order. We apply five time series analysis methods from nonlinear dynamics to determine the order of the processes and decide if the dynamics is deterministic or stochastic.

I. INTRODUCTION

Tremor denotes an involuntary oscillation of parts of the body. It is the most frequent movement disorder, see Refs. 1 and 2 for recent reviews on tremor. Tremor time series span a large range of different dynamical behaviors. The physiological tremor of healthy subjects represents a linear second order stochastic process driven by white noise originating from uncorrelated firing motoneurons.[3,4] The enhanced physiological tremor can either be described by a stochastic linear second order process driven by colored noise or a nonlinear stochastic delay differential equation depending on the degree of the contribution of a central pacemaker or of reflexes.[5,6]

Pathological tremors like essential and Parkinsonian tremor exhibit a nonlinear oscillation. The oscillation is not strictly periodic. There are at least three possible reasons for the deviation from a strictly periodic, limit cycle type of dynamics. First, deterministic chaos can be a source of apparently random behavior. Therefore, the processes have to be at least of third order. Second, the processes might be nonlinear stochastic oscillators, described by a second order differential equation with dynamical noise which is assumed to be additive. Third, the variability may result from nonstationarity in terms of time dependent parameters of the process. Formally, such processes could be described by high-dimensional dynamical systems.[7,8]

To investigate whether a second order stochastic, a third order deterministic or a high-dimensional process underlies the measured time series, we apply various methods from linear and nonlinear dynamics to time series recorded from patients suffering from essential and Parkinsonian tremor. Spectral analysis confirms the visual impression from the data that the processes represent a nonlinear oscillation that is not strictly periodic. The analysis of the local slopes of the correlation integrals,[9] Poincaré sections and return maps give no evidence for a low dimensional deterministic dynamics. The analysis of the local divergence of nearby trajectories[10] suggests a stochastic dynamics. 'Deterministic versus

[a)]Corresponding author: electronic mail: jeti@fdm.uni-freiburg.de

stochastic'—plots[11] and the $\delta-\epsilon$ method[12] support the hypothesis that the processes are of second order and obey a nonlinear stochastic dynamics. Over all, the results suggest that the considered pathological tremors represent a nonlinear stochastic process of second order with additive dynamical noise. Here, we only present the results for one essential and one Parkinsonian tremor time series. Qualitatively identical and quantitatively similar results were obtained for a larger set of time series. The complete set of 10 time series is available at the WWW-address given in Sec. VII.

For medical data, it is a challenge to support the clinical differential diagnosis by time series analysis. To this aim features have to be extracted from the time series that capture different dynamical properties of different diseases. Promising results of such an attempt for pathological tremor data have been reported in Refs. 13 and 14 based on 15 time series of essential tremor and 25 time series of Parkinsonian tremor. We apply the features to a set of 75 essential tremor and 112 Parkinsonian tremor time series to evaluate whether the former result is reproducible for a larger sample. The results are disappointing. We discuss the reason for this.

The paper is organized as follows. In the following section, we introduce the tremor data used in the further investigations and give the results of their spectral analysis. In Sec. III we discuss the stochastic van der Pol oscillator. We will use this process in the following sections to investigate the behavior of the considered algorithms in the presence of a nonlinear, stochastic second order oscillatory process. In Sec. IV we discuss and apply various methods from nonlinear dynamics to the data. In Sec. V we give the results of a classification of essential tremor and Parkinsonian tremor based on earlier proposed features using a larger set of time series.

II. THE DATA AND THEIR SPECTRA

The time series are recordings of the acceleration of the hand measured by piezoresistive accelerometers attached to the dorsum of the out-stretched hand. The sampling rate is 1000 Hz. The data are recorded for 30 s yielding time series of length 30.000. For the analysis the time series were normalized to zero mean and unit variance. The time series were selected from a large sample with respect to two criteria. Since the performance of most time series analysis methods decreases with decreasing signal to noise ratio, we chose time series with a large signal to noise ratio. Since our goal is to decide between second order stochastic, third order deterministic or a high-dimensional nonstationary process, second, we chose time series that do not exhibit obvious nonstationarities like drifts and abrupt changes in amplitude or frequency. Such behaviors are usually caused by the recording technique or by disturbances and interruptions by the patient. All the remaining variability of the time series is regarded as part of the dynamics. The variability of the chosen time series is typical for the two forms of pathological tremors.

Figure 1 shows two segments of the data for the essential and Parkinsonian tremor time series. The smooth behavior of the time series indicates that the amount of observational noise is rather small for these type of data in contrast to data recorded from physiological tremor, see Ref. 4 for an example. Figure 2 shows the time series embedded in a three dimensional phase space following Taken's theorem.[15] As delay time τ we choose the first zero-crossing of the autocorrelation function. This results in $\tau=52$ sampling units for the essential tremor and $\tau=54$ for the Parkinsonian tremor time series. This delay time is identical to the delay time given by the first minimum of the mutual information.[16] This is not unexpected for oscillatory time series of the type considered here.[17]

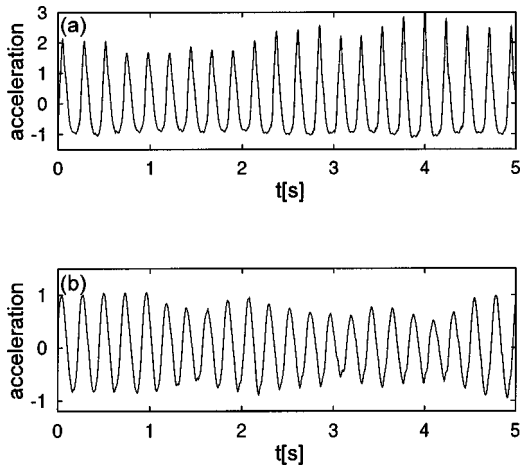

FIG. 1. Representative segments of the normalized time series. (a) Essential tremor, (b) Parkinsonian tremor.

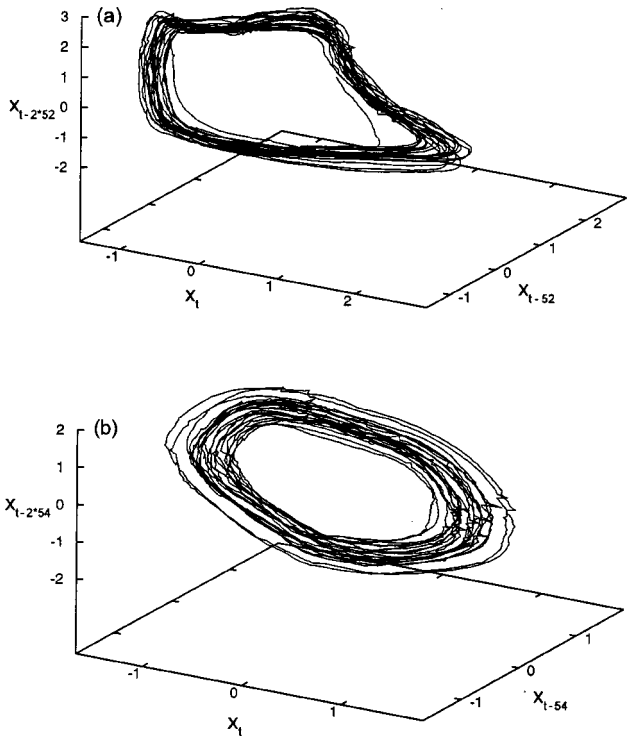

FIG. 2. Embedding of the time series in the reconstructed phase space. (a) Essential tremor, embedding delay $\tau=52$ sampling units. (b) Parkinsonian tremor, embedding delay $\tau=54$ sampling units.

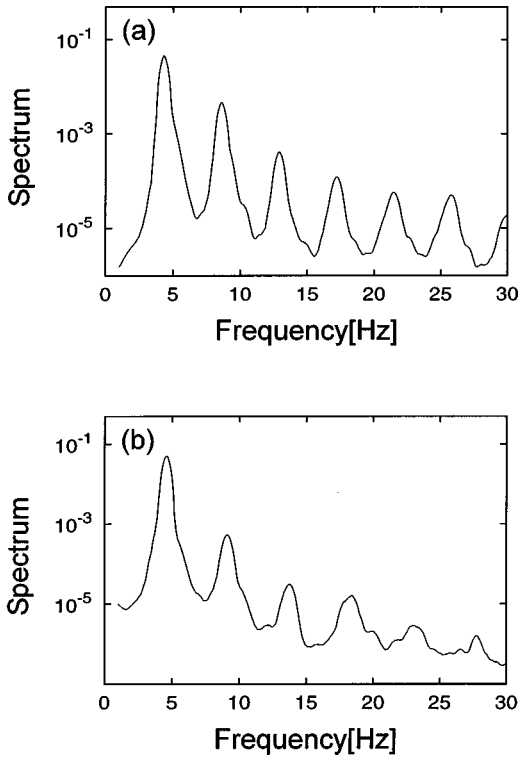

FIG. 3. Estimated spectra of the two tremors. (a) Essential tremor, (b) Parkinsonian tremor.

Figure 3 shows the estimated spectra based on the time series shown in Fig. 1. The estimation was based on smoothing the periodogram of the data, see Ref. 18 for details. The higher harmonics in the spectra indicate that the processes underlying the time series are not linear processes, but some kind of nonlinear oscillators.[19,20] The broadness of the peaks in Fig. 3 together with the time domain behavior displayed in Figs. 1 and 2 show that the processes are not (nonlinear) deterministic limit cycles, i.e., deterministic processes of order two. The deviation from a limit cycle type of behavior is the starting point for the following investigations. Apart from the trivial explanation that the tremors represent some nonstationary, effectively high-dimensional process, there are two possible alternatives that would be more distinctive: the variability can be caused by a deterministic chaotic process or by a nonlinear stochastic oscillator. The first alternative requires a third order dynamics; the second one a second order stochastic dynamics. Of course, more complicated dynamics might govern the time series, but we aim to identify the most economical description consistent with the data.

III. SIMULATED PROCESSES

Even linear stochastic processes of second order can produce a significant amount of variability in amplitude and frequency of the time series, see Fig. 1 in Ref. 8 for an example. Since we are dealing with nonlinear processes here, we use the stochastic van der Pol oscillator as an example of a nonlinear stochastic oscillator to evaluate the behavior of the below applied algorithms.

The van der Pol oscillator:[21]

$$\ddot{x}=\mu\,(1-x^2)\,\dot{x}-x, \quad \mu>0, \tag{1}$$

exhibits a stable limit cycle due to the amplitude dependent change of the sign of the damping term. We expose it to a random force of unit variance, leading to

$$\dot{x}_1=x_2, \tag{2}$$

$$\dot{x}_2=\mu\,(1-x_1^2)\,x_2-x_1+\epsilon, \tag{3}$$

where x_1 denotes the location and x_2 the velocity. Characteristic properties of the stochastic van der Pol oscillator and related perturbed limit cycles have been investigated in Refs. 22 and 23.

The integration of a stochastic differential equation like Eqs. (2) and (3) is not straightforward. This is due to the mathematical problems of evaluating integrals which involve the dynamical noise ϵ, see Ref. 24 for a brief introduction and Ref. 25 for a detailed discussion. Applying the same ideas underlying higher order integration schemes for deterministic differential equations like Runge–Kutta[26] to stochastic differential equations leads to hardly treatable stochastic integrals given in Ref. 27. Thus, only low order integration schemes can be used. The lowest order so-called Euler-scheme for Eqs. (2) and (3) is given by

$$x_1(t+\delta t)=x_1(t)+\delta t\,x_2(t), \tag{4}$$

$$x_2(t+\delta t)=x_2(t)+\delta t\,(\mu\,(1-x_1^2(t))\,x_2(t)-x_1(t))+\sqrt{\delta t}\,\epsilon(t). \tag{5}$$

In practice the necessity of using a low order scheme means that the integration step size δt is usually much smaller than the sampling interval Δt by which the time series is recorded. Here, we use $\delta t=0.001$ and $\Delta t=0.05$. The chosen sampling time Δt leads to a number of data points per mean period that is comparable to the respective number in the tremor data. The total number of simulated data points equals the number of data points in the measured data.

For examining the algorithms in presence of a chaotic process we use the Lorenz system[28] with parameters $\sigma=10$, $b=8/3$, and $r=28$, integrated by the fourth order Runge–Kutta method and sampled with $\Delta t=0.01$. Neither the van der Pol oscillator nor the Lorenz system are considered as possible models for pathological tremors. They serve as examples for the two possible types of dynamics, nonlinear second order stochastic dynamics and chaotic deterministic dynamics of third order. The simulated data are used to investigate the finite sample size properties of the algorithms to support an interpretation of the results for the measured data.

IV. NONLINEAR ANALYSIS

In this section we discuss the application of five methods from nonlinear dynamics to the pathological tremor time series. First, we apply quantities derived from the classical features of nonlinear dynamics, the correlation dimension, Poincaré and return maps and the largest Lyapunov exponent. Then, we apply more recently developed features, the deterministic versus stochastic (DVS) plots and the $\delta-\epsilon$ method.

A. Local slopes of correlation integrals

A fractal dimension of the attractor is one of the fascinating features of chaotic processes. One measure for this dimension is the correlation dimension D_2.[29,30] It is defined by

$$D_2 = \lim_{r \to 0} \frac{d \log C(r)}{d \log r}. \tag{6}$$

$C(r)$, the correlation integral, is given by

$$C(r) = \text{const} \sum_{i=1}^{N} \sum_{j=i+\mu}^{N} \Theta(r - |\vec{x}(i) - \vec{x}(j)|), \tag{7}$$

where $\vec{x}(i)$ denotes the states embedded in the reconstructed phase space,[15] $\Theta(.)$ the Heavyside function applied to count the number of pairs of points within a radius r and μ the Theiler correction employed to exclude temporally correlated points.[31]

This method has frequently been applied to measured data, but some of the results were a matter of debate, see, e.g., Refs. 32–35. A serious problem is that the existence of a scaling region for small radii r where Eq. (6) holds may not be assumed but has to be established. Therefore, plots of local slopes of the logarithm of the correlation integrals in dependence on the logarithm of r can be investigated. Evidence for a fractal attractor is given if the local slopes are constant for a large enough range of small radii and do not change for higher embedding dimensions. Problems in estimating correlation dimensions caused by the finite length of data are discussed in Refs. 31 and 36. Effects of dynamical and observational noise are investigated in Ref. 37. A recent discussion of the various aspects of estimating correlation dimensions from data is given in Ref. 9.

To determine the time delay τ for the embedding, we evaluated the first zero crossing of the autocorrelation function and the first minimum of the mutual information. For the stochastic van der Pol oscillator and the measured time series this led to identical results. For the Lorenz system we chose the first minimum of the mutual information ($\tau=10$). We applied the Theiler correction[31] by excluding $\mu=500$ temporally correlated points of the time series in the calculation of the correlation integrals.

Figures 4(a) and 4(b) show the correlation integrals for embedding dimensions one to eight for the Lorenz system and the stochastic van der Pol oscillator with $\mu=5$. The results for the Lorenz system are in accordance with the expectation. A scaling region for small radii r is identifiable. Furthermore, the functional behavior of the local slopes of the correlation integrals for small r does not change for embedding dimensions $d \geqslant 3$. No such behavior can be observed for the stochastic van der Pol oscillator. The structured behavior in the neighborhood of $r=0.8$ is due to large scale behavior of the invariant set.

Figures 4(c) and 4(d) show the corresponding plots for the measured data. There is no indication for a low dimensional fractal attractor.

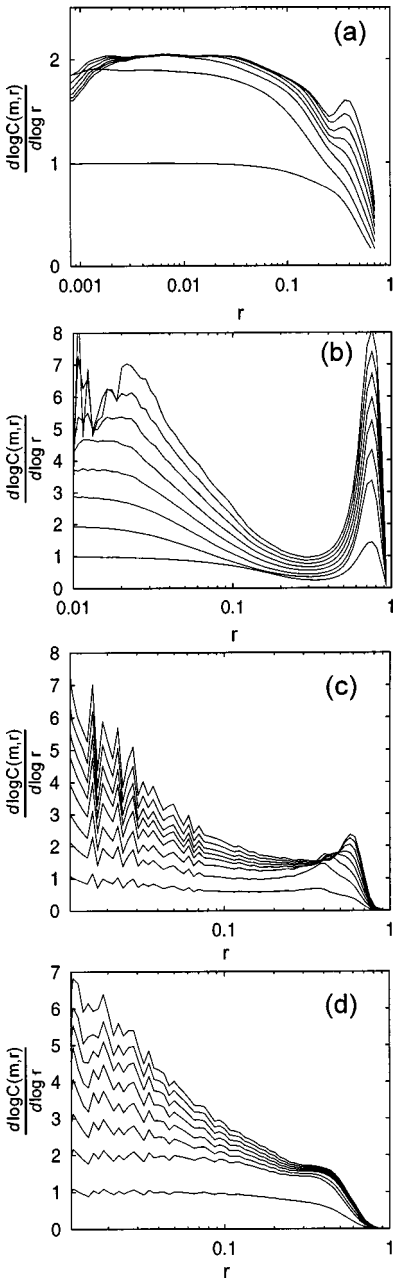

FIG. 4. Local slopes of the correlation integrals for simulated time series (a) Lorenz system, (b) stochastic van der Pol oscillator, and for the measured time series, (c) essential tremor, (d) Parkinsonian tremor.

B. Poincaré and return maps

Poincaré and return maps can be applied to reduce the dimension of the phase space and allow for an easier determination of a chaotic dynamics. A horseshoe behavior of the resulting map is a sufficient criterion to infer a chaotic behavior of the system.[19,38] For a Poincaré map, we chose the values of successive maxima of the time series. Return maps were formed by consecutive periods Δt_i of the time series. The periods were determined as time intervals between successive maxima measured in sampling units. Figure 5 shows the results for the measured time series. No indication of a horseshoe-behavior is present.

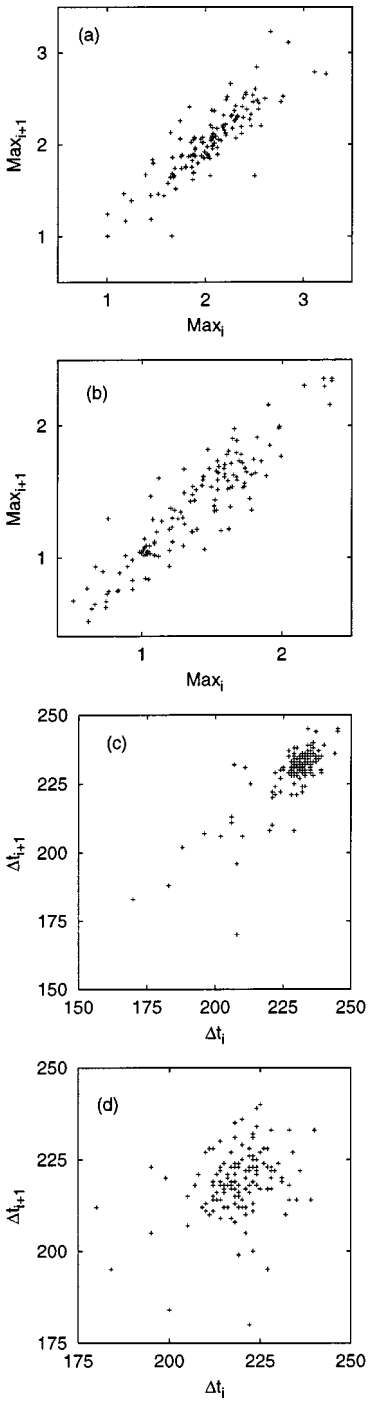

FIG. 5. Poincaré maps of the maxima (a) essential tremor, (b) Parkinsonian tremor and return maps of consecutive periods Δt_i measured in sampling units (c) essential tremor, (d) Parkinsonian tremor.

C. Lyapunov exponents

A positive Lyapunov exponent is one of the hallmarks of chaos. The local exponential divergence of nearby trajectories in chaotic systems lead to the sensitivity of the trajectories against small changes in the initial values. Different algorithms have been proposed to estimate the largest Lyapunov exponent or even their complete spectrum from measured data. The first type of algorithm investigates explicitly whether the time evolution of nearby trajectories over a certain fixed interval is a diverging or decaying exponential or a constant.[39] The second type of algorithms examines the tangent space of the dynamics.[40,41] Both types of algorithms assume that there is an exponentially separating behavior of nearby trajectories. However, also in stochastic dynamical systems nearby trajectories diverge.[42] Since these systems locally behave like Brownian motion, the separation follows a square root law. For a discussion of the notion of a positive Lyapunov exponent for stochastic systems, see Refs. 43 and 44 and references cited therein.

It has been shown that the above-mentioned algorithms can signal a spurious positive Lyapunov exponent when applied to stochastic systems.[45–49] The reason is that they assume an exponential behavior and effectively determine the parameter of the exponential from two points. The situation is similar to that for estimating correlation dimensions from correlation integrals discussed in the previous section: The exponential divergence may not be assumed but this functional form has to be established.

Generalizing ideas presented in Ref. 50, algorithms have been proposed to trace the behavior of nearby trajectories over time.[10,51] If this behavior is exponentially divergent it indicates a positive Lyapunov exponent. Another characteristic behavior can be found for Brownian motion. Here the divergence follows a square-root power law. These different types of separation behavior can be decided on by regarding it with a logarithmic, respectively linear scale of the time axis, where the different scaling behaviors can be identified. For time continuous nonlinear stochastic processes the square-root divergence behavior can only be expected for time scales where the Brownian motion like diffusion dominates the deterministic drift. This only holds for times in the order of the integration time step δt (see Sec. III) and smaller. Thus, in general, it can not be expected to be observed on the time scale of sampling. In fact, we neither observed it for the stochastic van der Pol oscillator nor for the measured time series.

In the following we use the algorithm suggested in Ref. 10. For initial neighborhoods $\mathcal{U}_i, i=1,\ldots,N$ of size ϵ in a m dimensional reconstructed phase space the quantity

$$S(\epsilon,m,t)=\left\langle \ln\left(\frac{1}{|\mathcal{U}_i|} \sum_{\vec{x}(j)\in\mathcal{U}_i} |\vec{x}(i+t)-\vec{x}(j+t)| \right) \right\rangle_i \qquad (8)$$

is evaluated in dependence on t. Similar to the local slopes for the correlation integrals, discussed above, we use local slopes of $S(\epsilon,m,t)$ to investigate if an exponential divergence is present. Since $S(\epsilon,m,t)$ behaves rather smoothly in dependence on t, the local slopes can be calculated reliably from three points. The information gained from the resulting plots is twofold. First, if the local slopes are positive and constant a chaotic dynamics is indicated. Second, the embedding dimension starting from which the course of the resulting curves does not change significantly indicates the order of the process.

Figures 6(a) and 6(b) show the resulting plots for the Lorenz system and Figs. 6(c) and 6(d) for the stochastic van der Pol oscillator with $\mu=5$ for embedding dimensions one to four and different sizes ϵ of the initial neighborhoods $\mathcal{U}_i$ $\times(\epsilon=0.02,0.026,0.034,0.044)$. For the Lorenz system, the re-

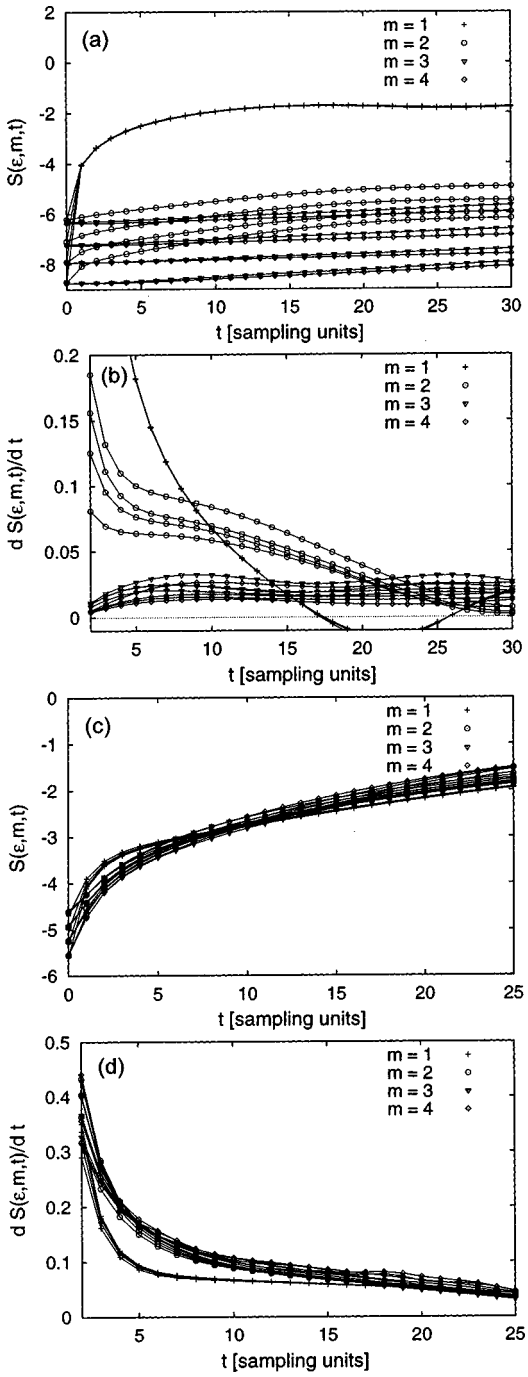

FIG. 6. Local divergence of initially nearby trajectories for the Lorenz system and the stochastic van der Pol oscillator for different sizes ϵ of the neighborhoods and embedding dimension $m=1,\ldots,4$. $+$: $m=1$, $\bigcirc$: $m=2$, $\triangledown$: $m=3$, $\diamond$: $m=4$. Lorenz system: (a) $S(\epsilon,m,t)$, see Eq. (8), (b) Local slopes of $S(\epsilon,m,t)$. Stochastic van der Pol oscillator: (c) $S(\epsilon,m,t)$, (d) Local slopes of $S(\epsilon,m,t)$.

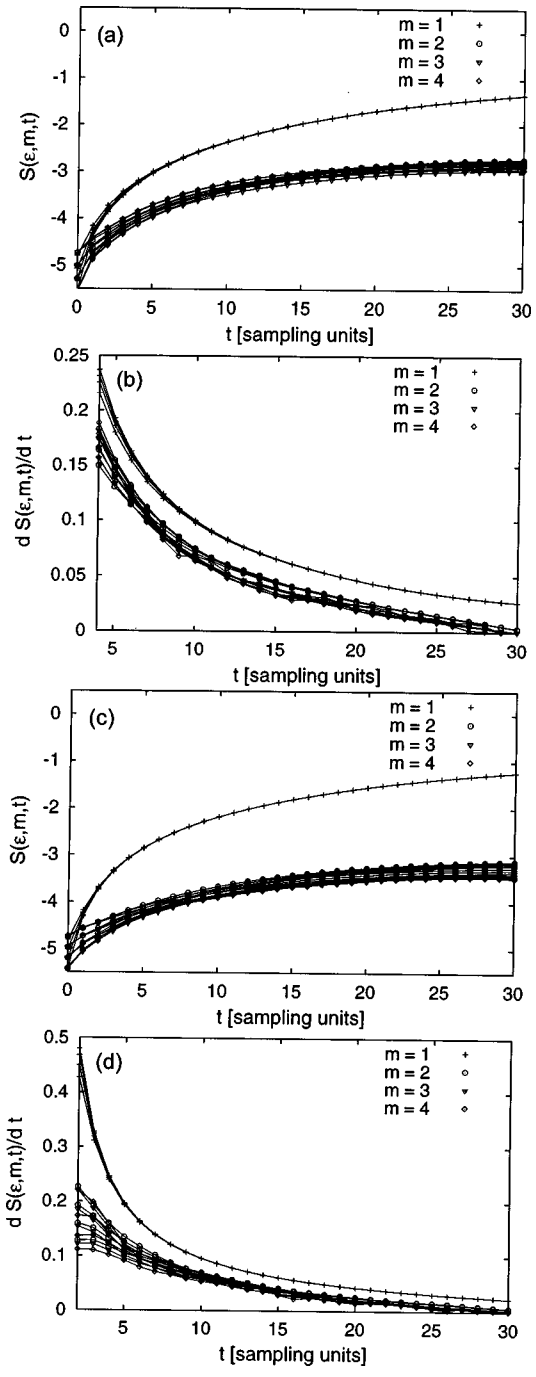

FIG. 7. Local divergence of initially nearby trajectories for the tremor time series. Essential tremor: (a) $S(\epsilon,m,t)$, (b) Local slopes of $S(\epsilon,m,t)$. Parkinsonian tremor: (c) $S(\epsilon,m,t)$, (d) Local slopes of $S(\epsilon,m,t)$.

sults exhibit the expected constant positive slope of $S(\epsilon,m,t)$ for embedding dimension three and larger [Fig. 6(b)]. For the stochastic van der Pol oscillator initially nearby trajectories also diverge, but not exponentially. The second order of this process is reflected by the invariance of the resulting curve for embedding dimension $m\geqslant 2$.

Figure 7 displays the results for the time series of the pathological tremors. The invariance of the resulting curve for embedding dimension $m\geqslant 2$ indicates a second order process. The nonexponential divergence of initially nearby trajectories indicate a stochastic dynamics.

D. Deterministic versus stochastic plots

Deterministic versus stochastic (DVS) plots were introduced in Ref. 11 and further discussed in Ref. 52. For different embedding dimensions, this method applies local linear predictions of the time series using different large neighborhoods for the local linear modeling and evaluates the mean prediction error. The information provided by this method is twofold. First, for sufficiently high embedding di-

mensions, nonlinear deterministic, nonlinear stochastic and linear stochastic processes result in different appearances of the DVS plots. For nonlinear deterministic processes the prediction error approaches zero for small neighborhoods and increases monotonically. For linear stochastic processes, the prediction errors should be largest for the smallest neighborhoods and decrease monotonically. Depending on the amount of dynamical noise and the degree of nonlinearity, nonlinear stochastic processes show either a minimum error in an intermediate size of neighborhoods or a monotonically increasing prediction error that does not reach zero for small neighborhoods.

Second, the order of the process can be inferred. For embedding dimensions larger than the true order, the prediction errors should not decrease any further and the functional form of the prediction errors in dependence on the size of the neighborhoods should not change anymore.

Figure 8 shows the DVS plots for the Lorenz system and the stochastic van der Pol oscillator. The results for the Lorenz system [Fig. 8(a)] exhibit the expected behavior. For embedding dimensions of three and larger the prediction errors reaches zero for small neighborhoods. For the stochastic van der Pol oscillator, the results for weak [$\mu=1$, Fig. 8(b)] and intermediate [$\mu=5$, Fig. 8(c)] degree of nonlinearity are given reproducing the two possible behaviors for nonlinear stochastic dynamics discussed above. The invariance of the functional dependence of the prediction errors on the size of the neighborhoods for embedding dimensions of two and larger excludes the possibility of an underlying chaotic process since this would require at least a dimension of three for continuous time dynamical systems considered here.

Additive observational noise poses severe problems on modeling and predicting time series.[4] It leads to an underestimation of the functional relationship between past and present values of the time series if not taken into account by the fitted model. For the DVS plots a decreased prediction performance is expected. Figure 8(d) displays the resulting DVS plots for the Lorenz system with additive white noise. The standard deviation of the noise is 1% of the standard deviation of the time series. This signal to noise ratio is larger than that of the measured time series. Compared to noise free case, Fig. 8(a), the curves do not reach zero prediction error for small ϵ for embedding dimension $m \leqslant 3$ anymore. But, the difference between the curve for $m=2$ and curves for $m \geqslant 3$ persists.

Figure 9 displays the results for the tremor data. Consistently, a second order process is suggested by the invariance of the functional form of the prediction error curves for higher embedding dimensions. The nonlinearity of the processes is reflected by the increase of the prediction error for larger ϵ. For small ϵ the prediction error shows a tendency to increase. Thus, the DVS-plots give evidence for a stochastic nonlinear second order dynamics.

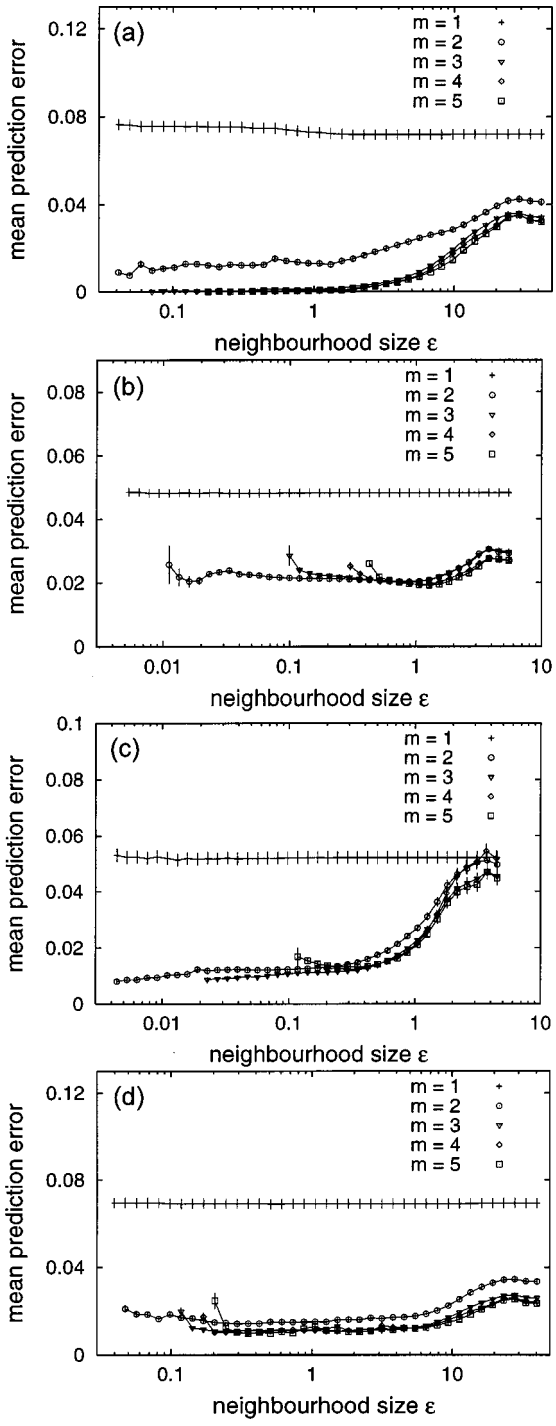

FIG. 8. DVS-plots for the simulated time series for embedding dimension one to five. +: $m=1$, ○: $m=2$, ▽: $m=3$, ◇: $m=4$ □: $m=5$. (a) Lorenz system, (b) stochastic van der Pol oscillator ($\mu=1$), (c) stochastic van der Pol oscillator ($\mu=5$), (d) Lorenz system with additive white noise. The standard deviation of the noise is 1% of the standard deviation of the time series.

E. $\delta-\epsilon$ method

The $\delta-\epsilon$ method was introduced in Ref. 12, where a detailed discussion of the method is given. The basic idea is that a deterministic dynamics embedded in a sufficiently high-dimensional state space should induce a continuous mapping from past to present states. Similarly to the DVS plots the size of the neighborhoods is increased to investigate the continuity. The size of the neighborhood of past states (δ) and the size of the resulting neighborhood of present states (ϵ) are plotted. For deterministic processes ϵ is expected to decrease to zero for decreasing δ for sufficiently high em-

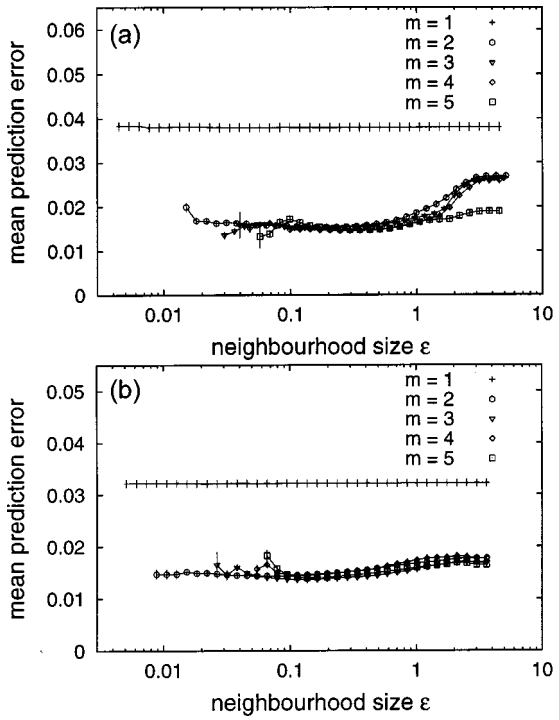

FIG. 9. DVS-plots for tremor time series for embedding dimension one to five. (a) Essential tremor, (b) Parkinsonian tremor.

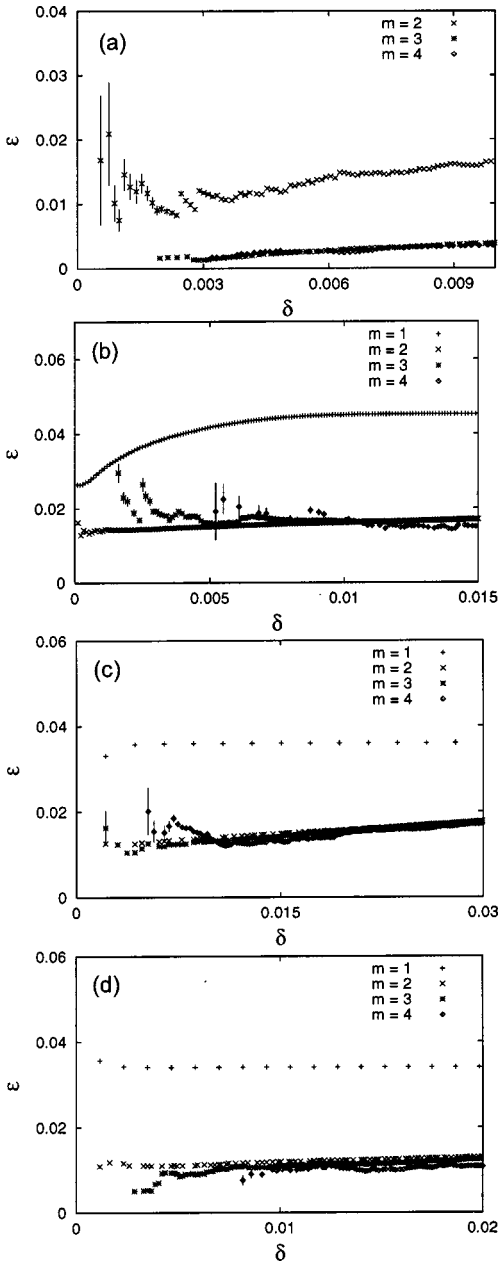

FIG. 10. Results for the $\delta-\epsilon$ method. (a) Lorenz system for embedding dimension two to four, (b) stochastic van der Pol oscillator ($\mu=5$) for embedding dimension one to four, (c) essential tremor, (d) Parkinsonian tremor.

bedding dimensions. For stochastic processes and processes which are covered by a significant amount of additive observational noise a non-zero intercept for ϵ is expected.

Figures 10(a) and 10(b) show the results for the Lorenz system and the stochastic van der Pol oscillator for $\mu=5$, see Eqs. (2) and (3). Extrapolating the resulting curves for the Lorenz system for embedding dimensions $m=3,4$ to zero yield the expected continuity. The results for the stochastic van der Pol oscillator indicate that in the case of stochastic processes for larger embedding dimensions the estimated ϵ for small δ show a large variance due to the curse of dimensionality. Figures 10(c) and 10(d) display the results for the two pathological tremors. Taking into account the variability of the estimated ϵ for small δ for the stochastic van der Pol oscillator in Fig. 10(b), the results for the pathological tremors confirm the results of the DVS plots in the previous section that a second order stochastic dynamics underlies the measured time series.

V. CLASSIFICATION OF PATHOLOGICAL TREMOR TIME SERIES REVISITED

The investigations in the preceding sections showed that the considered forms of pathological tremors are governed by nonlinear processes. It is a challenging task to investigate whether characteristics of the nonlinearities extracted from measured data are able to support the differential diagnosis between healthy and different types of pathological states usually performed by clinical observations, see Ref. 53 for a collection of examples from different biomedical domains.

For tremor time series the discrimination between essential and Parkinsonian tremor is of largest clinical importance. Visual inspection of clinically classified time series motivated us to investigate asymmetric behavior of the time series with respect to the direction of time and to a change of sign.[13,14] Algorithmically, the first was captured by a measure for time reversibility based on the difference of conditional expectations forward and backward in time:

$$\tilde{D}(y,\tau)=E\{x(t+\tau)|x(t)=y\}-E\{x(t-\tau)|x(t)=y\}. \tag{9}$$

$\tilde{D}(y,\tau)$ is estimated by a kernel estimator, see Ref. 13 for details. The dependence on y and τ was eliminated by forming:

$$\hat{D}(\tau)=\int dy\, \tilde{D}^2(y,\tau) \tag{10}$$

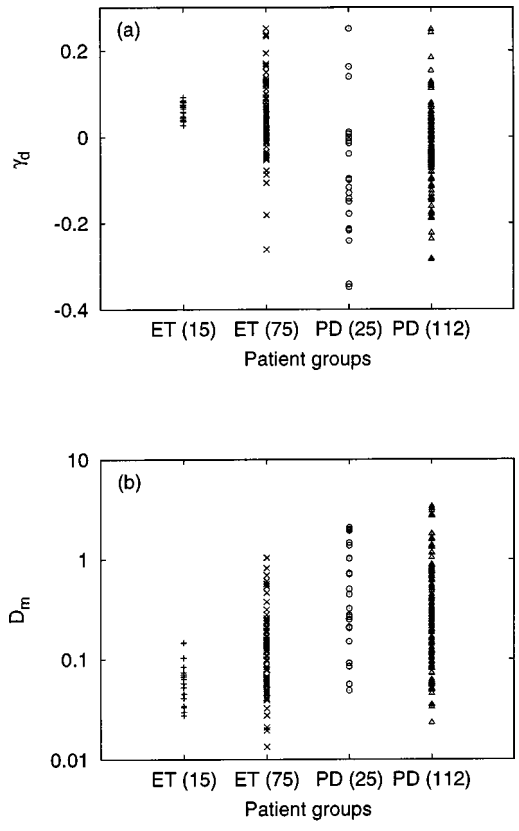

FIG. 11. Comparison of the distribution of classification features between the results based on small and on large samples of essential (ET) and Parkinsonian disease (PD) tremor time series. (a) Time reversibility, (b) Assymmetric decay of the autocorrelation function. +: essential tremor, small sample, ×: essential tremor, large sample ○: Parkinsonian tremor, small sample, △: Parkinsonian tremor, large sample.

and finally

$$\hat{D}_m = \max_{\tau} \hat{D}(\tau). \tag{11}$$

The asymmetry with respect to a change of sign was best captured by a measure for the asymmetric decay of the autocorrelation function. We calculated this by the difference γ_d of the absolute values of the first and the second maximum of the autocorrelation function.

In Refs. 13 and 14, we reported the classification results for a set of 15 essential and 25 Parkinsonian tremor time series. The classification rate was 75% for the measure of time reversibility and 90% for the asymmetric decay of the autocorrelation function. The classification rate based on the linear measures of amplitude and frequency is 30%, evaluated for a sample of 62 Parkinsonian and 52 essential tremor time series.[2] We repeated the nonlinear analysis for a larger set of 75 essential and 112 Parkinsonian clinically classified tremor time series. Figure 11 compares the former results based on the small sample with the new results based on the larger sample. Assuming the larger sample to be representative, it can be seen that the high classification rates of the former analysis were caused by a nonrepresentative sample of essential tremor time series. For both features the variance of their distributions is much smaller for the small sample. Thus, the variability of the processes is underestimated.

For the larger sample investigated here, the classification rate decreases to 30%, the same rate as found by the linear measures of amplitude and frequency.

VI. DISCUSSION

A decision on the order of a process and the type of dynamics—stochastic or deterministic—is difficult if the true order is large. Conclusive results can hardly be expected for an order of 5 or larger. In the case of the tremor time series considered here, the best treatable nontrivial case is given. In searching for the reason for variability of an nonlinear oscillator, the two simplest possibilities are chaotic determinism, calling for a third order process, or a stochastic oscillator of order two. The third possibility that some type of nonstationary, formally described as high-dimensional, process underlies the measured time series should be concluded if there is no conclusive decision between the former alternatives.

We first evaluated the correlation integrals, Poincaré and return maps and the largest Lyapunov exponent. Earlier investigations of the local slopes of the correlation integral and the Lyapunov exponents of Parkinsonian tremor time series performed in our group gave evidence for a chaotic dynamics.[54] To calculate the correlation integrals in these former investigations, we had chosen the time delay in the embedding equal to two sampling units. This is much smaller than values determined by recommended methods like mutual information or the autocorrelation function used here. Furthermore the Theiler correction[31] has not been applied. For the calculation of the Lyapunov spectrum we had applied an algorithm that is nowadays known to be able to yield positive Lyapunov exponents even for white noise. Therefore, we now doubt the validity of these former results. The results presented in this paper indicate that there is no finite correlation dimension and the analysis of the divergence behavior of nearby trajectories supports the hypothesis that a stochastic dynamics underlies the time series. Especially, the independence of the results for embedding dimensions $m \geqslant 2$ points to a second order dynamics. The Poincaré and return maps gave no evidence for a low dimensional chaotic dynamics.

The deterministic versus stochastic (DVS) plots gave strong evidence for a nonlinear stochastic process of second order underlying the time series of the considered types of pathological tremors. The $\delta - \epsilon$ method confirmed the results of the DVS plots. For the DVS plots and the $\delta - \epsilon$ method the characteristic behavior of the resulting curves gave information about the nature of the dynamics underlying the measured time series. For both these methods as for the divergence analysis, the embedding dimension starting form which the resulting curve does not change any more gives valuable information indicating a second order dynamics.

A final hint for nonchaotic second order oscillators governing the time series stems from the mutual information. In order to determine the time delay for the embedding we calculated both the mutual information and the autocorrelation function. For systems other than second order oscillators, it has been shown that the time lag of first minimum of the

mutual information differs from that of the first crossing of the autocorrelation function.[17] For all time series investigated here, they coincide.

We also applied the method of false nearest neighbors.[55,56] In simulation studies based on the stochastic van der Pol oscillator and the Lorenz system with additive observational noise we did not succeed to recover the correct order of the processes. The order was overestimated in both cases. For the measured time series the results were not conclusive.

In summary, a consistent interpretation of the different methods indicate that the variability of the oscillation of the pathological tremors is best described by a nonlinear stochastic second order process. The DVS plots appeared to be most informative for a discrimination between the two alternatives of a third order chaotic and a second order nonlinear stochastic process. Our findings contradict the suggestion[57] that the variability observed in the considered pathological tremors should be interpreted as caused by frequency and/or amplitude modulated harmonic oscillators.

Finally, we tried to reproduce the classification results for the two types of pathological tremor based on features that capture properties of the nonlinear dynamics reported in Refs. 13 and 14. Using a much larger sample of time series, we were not able to achieve the reported classification rates. The high classification rates reported in Refs. 13 and 14 were revealed to be caused by a nonrepresentative sample of the essential tremor time series. The attempt to classify medical time series based on extracted features assumes that the different diseases are actually different processes. For the two types of pathological tremors considered here there is evidence that there might by more similarities than substantial differences between the processes although the underlying pathologies are likely to be different.[58]

The decrease of the classification rates demonstrates the importance of evaluating classification features on a large representative sample preferably collected in prospective studies.

VII. DATA AVAILABILITY

The time series used in the above investigations and further essential and Parkinsonian tremor time are available at: http://phym1.physik.uni-freiburg.de/~jeti/path_tremor

ACKNOWLEDGMENTS

We gratefully acknowledge the use of the software package TISEAN provided by R. Hegger, H. Kantz and T. Schreiber (Ref. 59) which is available at http://www.mpipks-dresden.mpg.de/~tisean The calculation of the local slopes of the correlation integral, the divergence behavior of nearby trajectories and the Deterministic versus stochastic–plots were performed by the TISEAN software. Especially, we thank R. Hegger for adjusting parts of the software to our needs.

[1] R. Elble and W. Koller, *Tremor* (Johns Hopkins University Press, Baltimore, 1990).
[2] G. Deuschl, P. Krack, M. Lauk, and J. Timmer, J. Clinic. Neurophys. **13**, 110 (1996).
[3] J. Timmer, M. Lauk, W. Pfleger, and G. Deuschl, Biol. Cybern. **78**, 349 (1998).
[4] J. Timmer, Int. J. Bifurcation Chaos Appl. Sci. Eng. **8**, 1505 (1998).
[5] J. Timmer, M. Lauk, W. Pfleger, and G. Deuschl, Biol. Cybern. **78**, 359 (1998).
[6] B. Köster *et al.*, Neurosci. Lett. **241**, 135 (1998).
[7] T. Schreiber, Phys. Rev. Lett. **78**, 843 (1997).
[8] J. Timmer, Phys. Rev. E **58**, 5153 (1998).
[9] H. Kantz and T. Schreiber, *Nonlinear Time Series Analysis* (Cambridge Univ. Press, Cambridge, 1997).
[10] H. Kantz, Phys. Lett. A **185**, 77 (1994).
[11] M. Casdagli, J. R. Stat. Soc. B **54**, 303 (1991).
[12] D. Kaplan, Physica D **73**, 38 (1994).
[13] J. Timmer, C. Gantert, G. Deuschl, and J. Honerkamp, Biol. Cybern. **70**, 75 (1993).
[14] G. Deuschl, M. Lauk, and J. Timmer, Chaos **5**, 48 (1995).
[15] F. Takens, in *Dynamical Systems and Turbulence*, Lecture Notes in Mathematics, Vol. 898, edited by D. Rand and L. Young (Springer, Berlin, 1981), pp. 366–381.
[16] A. Fraser and H. Swinney, Phys. Rev. A **33**, 1134 (1986).
[17] A. Fraser and H. Swinney, Physica D **34**, 391 (1989).
[18] J. Timmer, M. Lauk, and G. Deuschl, Electroencephalogr. Clin. Neurophysiol. **101**, 461 (1996).
[19] A. Lichtenberg and M. Lieberman, *Regular and Stochastic Motion*, Applied Mathematical Sciences, Vol. 38 (Springer, New York, 1992).
[20] G. Giacaglia, *Perturbation Methods in Non-Linear Systems*, Applied Mathematical Sciences, Vol. 8 (Springer, New York, 1972).
[21] B. van der Pol, Philos. Mag. **43**, 177 (1922).
[22] C. Kurrer and K. Schulten, Physica D **50**, 311 (1991).
[23] H. Leung, Physica A **221**, 340 (1995).
[24] P. Kloeden, E. Platen, and H. Schurz, Int. J. Bifurcation Chaos Appl. Sci. Eng. **1**, 277 (1991).
[25] P. Kloeden and E. Platen, *Numerical Solution of Stochastic Differential Equations*, Applications of Mathematics, Vol. 23 (Springer, New York, 1992).
[26] W. Press, B. Flannery, S. Saul, and W. Vetterling, *Numerical Recipes* (Cambridge Univ. Press, Cambridge, 1992).
[27] J. Honerkamp, *Stochastic Dynamical Systems* (VCH, New York, 1993).
[28] E. Lorenz, J. Atmos. Sci. **20**, 130 (1963).
[29] P. Grassberger and I. Procaccia, Physica D **9**, 189 (1983).
[30] P. Grassberger and I. Procaccia, Phys. Rev. Lett. **50**, 346 (1983).
[31] J. Theiler, Phys. Rev. A **34**, 2427 (1986).
[32] C. Nicolis and G. Nicolis, Nature (London) **311**, 529 (1984).
[33] P. Grassberg, Nature (London) **323**, 609 (1986).
[34] C. Nicolis and G. Nicolis, Nature (London) **326**, 523 (1987).
[35] P. Grassberger, Nature (London) **326**, 524 (1987).
[36] A. Jedynak, M. Bach, and J. Timmer, Phys. Rev. E **50**, 1770 (1994).
[37] H. Kantz and T. Schreiber, Chaos **5**, 143 (1995).
[38] H. Schuster, *Deterministic Chaos* (VCH, Weinheim, 1989).
[39] A. Wolf, J. Swift, H. Swinney, and L. Vastano, Physica D **16**, 285 (1985).
[40] M. Sano and Y. Sawada, Phys. Rev. Lett. **55**, 1082 (1985).
[41] J.-P. Eckmann, S. Kamphorst, D. Ruelle, and S. Ciliberto, Phys. Rev. A **34**, 4971 (1986).
[42] W. Ebeling, H. Herzel, and L. Schimansky-Geier, in *From Chemical to Biological Organization*, No. 39 in *Springer Series in Synergetics*, edited by M. Markus (Springer, Heidelberg, 1988), pp. 166–176.
[43] *Lyapunov Exponents*, Lecture Notes in Statistics, Vol. 1486, edited by L. Arnold, H. Crauel, and J. Eckmann (Springer, New York, 1991).
[44] L. Schimansky-Geier and H. Herzel, J. Stat. Phys. **1/2**, 141 (1993).
[45] M. Dämmig and F. Mitschke, Phys. Lett. A **178**, 385 (1993).
[46] F. Mitschke and M. Dämmig, Int. J. Bifurcation Chaos Appl. Sci. Eng. **3**, 693 (1993).
[47] J. Fell, J. Röschke, and P. Beckmann, Biol. Cybern. **69**, 139 (1993).
[48] T. Tanaka, K. Aihara, and M. Taki, Phys. Rev. E **54**, 2122 (1996).
[49] T. Tanaka, K. Aihara, and M. Taki, Physica D **111**, 42 (1998).
[50] H. Herzel and W. Ebeling, Biomed. Biochem. Acta **8/9**, 941 (1990).
[51] M. Rosenstein, J. Collins, and C. DeLuca, Physica D **65**, 117 (1993).
[52] M. Casdagli and A. Weigend, in *Time Series Prediction*, Studies in the Science of Complexity, Santa Fe Institute, edited by A. Weigend and M. Gerschenfeld (Addison-Wesley, Reading, 1994), Vol. XV, pp. 347–366.

[53] *Dynamical Disease*, Mathematical Analysis of Human Illness, edited by J. Belair, L. Glass, U. an der Heiden, and J. Milton (American Institute of Physics, Woodbury, New York, 1995).
[54] C. Gantert, J. Honerkamp, and J. Timmer, Biol. Cybern. **66**, 479 (1992).
[55] M. Kennel and S. Isabelle, Phys. Rev. A **46**, 3111 (1992).
[56] H. Abarbanel, *Analysis of Observed Chaotic Data* (Springer, Berlin, 1996).
[57] M. Gresty and D. Buckwell, J. Neurol. Neurosur. Psych. **53**, 976 (1990).
[58] C. Lücking *et al.*, Adv. Neurology **80**, 335 (1999).
[59] R. Hegger, H. Kantz, and T. Schreiber, Chaos **9**, 413 (1999).